

OBSERVATIONS OF THE INFRARED TRIPLET OF SINGLY IONIZED CALCIUM

JEFFREY L. LINSKY

Joint Institute for Laboratory Astrophysics, University of Colorado, Boulder, Colo., U.S.A.*

RICHARD G. TESKE

Department of Astronomy, University of Michigan, Ann Arbor, Mich., U.S.A.

and

CAROL W. WILKINSON

Harvard College Observatory, Cambridge, Mass., U.S.A.

(Received 11 September, 1969)

Abstract. Observations are presented of the Ca II infrared triplet (8498 Å, 8542 Å, and 8662 Å) at three positions on the solar disk to make possible direct analyses of the lines and comparisons with theoretical computations. The source functions for the two strongest lines (8542 Å and 8662 Å) are equal at those heights corresponding to the wings of the lines ($|\Delta\lambda| > 0.4 \text{ Å}$) but not to those of the cores. We suggest that the apparent source function inequality in the cores is due to limb darkening caused by inhomogeneities in the chromosphere.

1. Introduction

The H and K resonance lines of singly-ionized calcium provide convenient but poorly understood probes of the solar chromosphere. Complicating the solution of the statistical equilibrium and radiative transfer equations for these lines are considerations of complex geometry, systematic high velocity motions, and the spectral redistribution of scattered photons for which complete redistribution in the rest frame of the observer is probably a poor approximation (Skumanich, 1969). In addition, a two-level approximation for the calcium ion is known (Jefferies, 1960; Athay and Zirker, 1962; Linsky, 1968) to yield emergent line profiles which are considerably in error.

A more adequate representation of the Ca II ion must include the metastable $3^2D_{3/2}$ and $3^2D_{5/2}$ levels in addition to the ground state $4^2S_{1/2}$ level and the $4^2P_{1/2}$ and $4^2P_{3/2}$ excited levels. The transitions $4^2P_{1/2} \rightarrow 4^2S_{1/2}$ and $4^2P_{3/2} \rightarrow 4^2S_{1/2}$ yield the H and K lines at 3968 Å and 3933 Å, respectively, while the subordinate transitions $4^2P_{1/2} \rightarrow 3^2D_{3/2}$, $4^2P_{3/2} \rightarrow 3^2D_{5/2}$, and $4^2P_{3/2} \rightarrow 3^2D_{3/2}$ give the triplet at 8662 Å, 8542 Å, and 8498 Å, respectively. We thus have available five lines, whose line center opacities differ by nearly three orders of magnitude, and which are formed at different heights in the lower chromosphere. These five lines may then be compared with statistical equilibrium solutions of a five-level Ca II ion in order to infer physical properties of the lower chromosphere. By including the infrared triplet lines in such a synthetic approach as additional constraints upon acceptable solutions, it should be

* Of the National Bureau of Standards and University of Colorado.

easier to distinguish among possible models of the chromosphere and to test the adequacy of the many assumptions used in computing the line profiles.

In addition, profiles of the infrared lines may be inverted to yield source functions and line broadening parameters as a function of line center optical depths. This type of analytic approach has been employed by Waddell (1962) and by Curtis and Jefferies (1967) on the Na D lines and by Waddell (1963) on the Mg I b lines. One aim of this paper is to obtain data which are suitable for such work.

With these goals in mind we set out to obtain mean profiles of the infrared lines at low spatial resolution, 2×60 arcsec, with sufficient spectral purity and with low scattered light contamination, to provide accurate residual intensities and limb darkening data. Earlier observations of these lines, for example, the work of Minnaert *et al.* (1940), Mohler *et al.* (1962), and Delbouille and Roland (1963) exhibit central intensities larger than those we observe due to insufficient spectral resolution or scattered light. The more recent observations of De Jager and Neven (1967) are of lower spectral resolution than ours and also exhibit systematically larger central intensities. Below we describe the observations in detail and deduce some general properties of the line source functions from the data.

2. The Observations

Profiles of the three infrared lines were obtained photoelectrically in quiet regions of the chromosphere using the vacuum spectrograph and solar tower of the McMath-Hulbert Observatory. These data are the first obtained on this telescope using a double pass configuration similar to that described by Pierce (1964). With the slit widths employed, 150μ for the entrance and exit slits, instrumental resolving power exceeded 200000, or better than 0.042 \AA in these lines. No corrections for finite instrumental bandwidth were deemed necessary for these broad lines.

Profiles of the lines were obtained at $\mu = 1.0, 0.5,$ and 0.3 between October 1966 and February 1967. The spectral scans extend to $20\text{--}25 \text{ \AA}$ on either side of the lines to establish an accurate continuum. In addition, the cores of the lines were scanned either two or three times at a much slower speed and the scattered light for the entire profile was scanned at a more rapid speed. In these latter scans the calcium absorption lines are seen as depressions in the scattered light level.

In reducing the data from the analog record, the dark current was presumed to vary linearly over the course of a 30 minute scan and the continuum was interpolated among measured points by parabolic segments. The data were then corrected for scattered light as measured at each wavelength and the resultant core residual intensities were obtained every 0.02 \AA . These residual intensities refer to the interpolated line center continua at $\mu = 1.0$ and are corrected for limb darkening using the data of David and Elste (1962). As the continuum is quite 'clean' in this region of the solar spectrum, the primary sources of error are random fluctuations on a short time scale and very slow changes in atmospheric transmission. We estimate the magnitude of these errors to be 0.003 in absolute value about the mean residual intensities.

TABLE I
Residual intensities of the 8542 Å line

$\Delta\lambda$	$\mu=1.0$			$\mu=0.5$			$\mu=0.3$		
	Blue	Red	Mean	Blue	Red	Mean	Blue	Red	Mean
0.00	0.179	0.179	0.179	0.151	0.151	0.151	0.132	0.132	0.132
0.02	0.179	0.180	0.180	0.152	0.153	0.152	0.132	0.132	0.132
0.04	0.182	0.184	0.183	0.154	0.156	0.155	0.133	0.134	0.134
0.06	0.187	0.189	0.188	0.158	0.161	0.160	0.136	0.137	0.137
0.08	0.191	0.198	0.195	0.162	0.168	0.165	0.140	0.141	0.141
0.10	0.203	0.207	0.205	0.171	0.176	0.174	0.145	0.146	0.146
0.12	0.217	0.218	0.218	0.185	0.186	0.186	0.153	0.153	0.153
0.14	0.237	0.235	0.236	0.201	0.199	0.200	0.165	0.165	0.165
0.16	0.256	0.252	0.254	0.223	0.214	0.218	0.179	0.175	0.177
0.18	0.276	0.275	0.275	0.242	0.233	0.238	0.193	0.188	0.191
0.20	0.301	0.304	0.302	0.265	0.246	0.256	0.210	0.205	0.207
0.22	0.317	0.329	0.323	0.287	0.272	0.278	0.233	0.224	0.228
0.24	0.333	0.358	0.346	0.306	0.299	0.303	0.258	0.247	0.253
0.26	0.349	0.383	0.366	0.327	0.325	0.326	0.282	0.274	0.278
0.28	0.366	0.399	0.383	0.344	0.350	0.347	0.300	0.300	0.300
0.30	0.381	0.412	0.397	0.359	0.374	0.367	0.317	0.325	0.321
0.32	0.394	0.424	0.409	0.372	0.383	0.378	0.336	0.348	0.342
0.34	0.404	0.434	0.419	0.386	0.404	0.395	0.352	0.363	0.358
0.36	0.414	0.443	0.428	0.398	0.416	0.407	0.368	0.378	0.373
0.38	0.424	0.450	0.437	0.408	0.424	0.416	0.380	0.388	0.384
0.40	0.431	0.457	0.444	0.418	0.432	0.425	0.390	0.397	0.394
0.42	0.441	0.462	0.452	0.425	0.439	0.432	0.401	0.406	0.404
0.44	0.445	0.466	0.456	0.433	0.445	0.439	0.409	0.413	0.410
0.46	0.451	0.473	0.462	0.439	0.451	0.445	0.415	0.418	0.417
0.48	0.458	0.479	0.468	0.446	0.456	0.451	0.421	0.424	0.423
0.52	0.467	0.488	0.478	0.457	0.465	0.461	0.431	0.433	0.432
0.56	0.478	0.496	0.488	0.467	0.474	0.470	0.438	0.441	0.440
0.60	0.488	0.507	0.497	0.476	0.480	0.478	0.445	0.448	0.448
0.64	0.497	0.514	0.506	0.483	0.488	0.485	0.453	0.455	0.454
0.68	0.504	0.521	0.513	0.490	0.493	0.491	0.458	0.460	0.459
0.72	0.512	0.527	0.520	0.496	0.499	0.497	0.464	0.466	0.465
0.76	0.520	0.534	0.527	0.502	0.504	0.503	0.469	0.470	0.470
0.80	0.527	0.545	0.536	0.508	0.509	0.509	0.473	0.474	0.474
0.84	0.534	0.552	0.543	0.514	0.521	0.517	0.478	0.478	0.478
0.88	0.540	0.559	0.550	0.519	0.527	0.523	0.482	0.482	0.482
0.92	0.547	0.566	0.557	0.524	0.532	0.528	0.486	0.486	0.486
0.96	0.553	0.572	0.562	0.531	0.537	0.534	0.491	0.486	0.488
1.00	0.556	0.576	0.566	0.536	0.541	0.539	0.494	0.490	0.492
1.10	0.571			0.547	0.551	0.549	0.501	0.500	0.500

In Tables I, II, and III the resultant residual intensities are given for the red and blue wings of each line. Also given are the means of the two wings corrected for the absorption line in the blue wing of the 8662 Å line. Those data which are affected by this additional absorption are placed in parentheses. The residual intensities at the center of the disk ($\mu=1.0$) are plotted in Figure 1 together with the residual intensities of the 8662 Å line at $\mu=0.5$. The wavelength scale $\Delta\lambda$ is measured relative

TABLE II
Residual intensities of the 8662 Å line

$\Delta\lambda$	$\mu = 1.0$			$\mu = 0.5$			$\mu = 0.3$		
	Blue	Red	Mean	Blue	Red	Mean	Blue	Red	Mean
0.00	0.176	0.176	0.176	0.146	0.146	0.146	0.129	0.129	0.129
0.02	0.178	0.178	0.178	0.147	0.149	0.148	0.130	0.130	0.130
0.04	0.183	0.183	0.183	0.146	0.153	0.149	0.131	0.131	0.131
0.06	0.189	0.191	0.190	0.153	0.159	0.155	0.134	0.134	0.134
0.08	0.194	0.201	0.198	0.165	0.165	0.165	0.140	0.139	0.140
0.10	0.205	0.212	0.208	0.176	0.175	0.175	0.146	0.147	0.147
0.12	0.222	0.221	0.222	0.194	0.186	0.190	0.156	0.156	0.156
0.14	0.243	0.236	0.240	0.213	0.197	0.205	0.169	0.168	0.169
0.16	0.261	0.250	0.255	0.234	0.217	0.226	0.185	0.183	0.184
0.18	0.277	0.270	0.274	0.246	0.235	0.241	0.199	0.200	0.200
0.20	(0.288)	0.294	0.293	(0.258)	0.248	0.262	(0.213)	0.217	0.217
0.22	(0.292)	0.319	0.314	(0.260)	0.283	0.290	(0.226)	0.237	0.237
0.24	(0.281)	0.349	0.337	(0.266)	0.309	0.313	(0.242)	0.262	0.260
0.26	(0.280)	0.379	0.361	(0.278)	0.338	0.339	(0.259)	0.294	0.288
0.28	(0.285)	0.397	0.377	(0.298)	0.367	0.364	(0.284)	0.319	0.316
0.30	(0.298)	0.413	0.394	(0.322)	0.390	0.384	(0.303)	0.342	0.344
0.32	(0.320)	0.424	0.407	(0.355)	0.406	0.400	(0.327)	0.363	0.366
0.34	(0.354)	0.435	0.419	(0.381)	0.420	0.414	(0.350)	0.386	0.386
0.36	(0.386)	0.445	0.429	(0.414)	0.432	0.427	(0.381)	0.401	0.401
0.38	(0.410)	0.453	0.439	0.430	0.442	0.436	(0.401)	0.414	0.413
0.40	(0.427)	0.462	0.449	0.439	0.451	0.445	(0.416)	0.424	0.423
0.42	(0.442)	0.468	0.457	0.451	0.459	0.455	(0.426)	0.432	0.431
0.44	0.451	0.476	0.463	0.457	0.465	0.461	0.435	0.437	0.436
0.46	0.461	0.481	0.471	0.464	0.470	0.467	0.442	0.441	0.442
0.48	0.466	0.486	0.476	0.470	0.475	0.472	0.448	0.448	0.448
0.52	0.478	0.495	0.487	0.479	0.484	0.482	0.459	0.458	0.458
0.56	0.489	0.505	0.497	0.489	0.494	0.492	0.466	0.466	0.466
0.60	0.498	0.513	0.506	0.498	0.502	0.500	0.474	0.472	0.473
0.64	0.508	0.522	0.515	0.506	0.509	0.508	0.481	0.479	0.480
0.68	0.515	0.531	0.523	0.514	0.517	0.515	0.487	0.486	0.487
0.72	0.533	0.545	0.539	0.521	0.524	0.523	0.493	0.493	0.493
0.76	0.541	0.552	0.547	0.528	0.529	0.529	0.500	0.498	0.499
0.80	0.546	0.559	0.553	0.534	0.535	0.535	0.504	0.504	0.504
0.84	0.551	0.569	0.560	0.539	0.542	0.541	0.509	0.509	0.509
0.88		0.575		0.545	0.548	0.541	0.513	0.513	0.513
0.92		0.583		0.550	0.555	0.553	0.515	0.518	0.516
0.96		0.591		0.555	0.562	0.558	0.519	0.521	0.520
1.00		0.597		0.559	0.568	0.563	0.524	0.524	0.524
1.10				0.573	0.584	0.579		0.526	

to the wavelength of minimum residual intensity rather than to the true rest line center because of the difficulty in establishing an absolute wavelength scale in the slow scans of the line core regions. Since 1 km/sec motion corresponds to a 0.03 Å displacement at these wavelengths, the apparent line centers could be red shifted by 0.03 Å if systematic motions in the infrared lines are similar to those observed on the average in K_3 .

TABLE III
Residual intensities of the 8498 Å line

$\Delta\lambda$	$\mu = 1.0$			$\mu = 0.5$			$\mu = 0.3$		
	Blue	Red	Mean	Blue	Red	Mean	Blue	Red	Mean
0.00	0.257	0.257	0.257	0.235	0.235	0.231	0.211	0.211	0.211
0.02	0.258	0.258	0.258	0.236	0.238	0.237	0.212	0.212	0.212
0.04	0.261	0.262	0.261	0.238	0.243	0.241	0.216	0.217	0.216
0.06	0.268	0.268	0.268	0.246	0.251	0.249	0.222	0.224	0.223
0.08	0.277	0.280	0.279	0.251	0.262	0.257	0.231	0.235	0.233
0.10	0.294	0.291	0.293	0.272	0.278	0.275	0.245	0.248	0.247
0.12	0.310	0.309	0.309	0.295	0.295	0.295	0.266	0.264	0.265
0.14	0.335	0.328	0.331	0.316	0.318	0.317	0.294	0.277	0.285
0.16	0.363	0.353	0.358	0.342	0.341	0.342	0.315	0.298	0.306
0.18	0.379	0.383	0.381	0.367	0.364	0.366	0.341	0.323	0.332
0.20	0.406	0.419	0.412	0.396	0.393	0.395	0.367	0.354	0.360
0.22	0.426	0.456	0.441	0.417	0.427	0.422	0.386	0.377	0.382
0.24	0.443	0.481	0.462	0.434	0.458	0.446	0.407	0.405	0.406
0.26	0.459	0.497	0.478	0.451	0.481	0.466	0.425	0.431	0.423
0.28	0.473	0.513	0.493	0.460	0.500	0.480	0.442	0.450	0.446
0.30	0.487	0.528	0.507	0.478	0.512	0.495	0.453	0.465	0.459
0.32	0.500	0.541	0.522	0.491	0.523	0.507	0.465	0.477	0.471
0.34	0.510	0.552	0.531	0.502	0.532	0.517	0.476	0.488	0.482
0.36	0.523	0.564	0.543	0.511	0.542	0.527	0.483	0.496	0.490
0.38	0.532	0.574	0.553	0.521	0.549	0.535	0.491	0.504	0.497
0.40	0.545	0.584	0.564	0.530	0.556	0.538	0.499	0.511	0.505
0.42	0.554	0.591	0.573	0.538	0.563	0.551	0.505	0.517	0.512
0.44	0.564	0.601	0.582	0.545	0.570	0.557	0.512	0.522	0.517
0.46	0.571	0.609	0.590	0.553	0.576	0.565	0.518	0.528	0.523
0.48	0.580	0.616	0.598	0.559	0.583	0.571	0.523	0.533	0.528
0.52	0.598	0.631	0.615	0.572	0.594	0.583	0.535	0.541	0.538
0.56	0.616	0.645	0.631	0.584	0.607	0.596	0.544	0.549	0.547
0.60	0.633	0.660	0.646	0.596	0.618	0.607	0.554	0.558	0.556
0.64	0.650	0.675	0.667	0.607	0.628	0.617	0.562	0.565	0.564
0.68	0.668	0.688	0.678	0.617	0.637	0.627	0.569	0.573	0.571
0.72	0.686	0.702	0.694	0.626	0.645	0.635	0.576	0.575	0.576
0.76	0.700	0.716	0.708	0.635	0.652	0.644	0.576	0.580	0.578
0.80	0.711	0.724	0.717	0.641	0.663	0.652	0.581		
0.84	0.722	0.735	0.728	0.647	0.670	0.658			
0.88	0.731	0.746	0.738	0.650	0.678	0.664			
0.92	0.732	0.755	0.744		0.686				
0.96		0.766							

From the data we may draw the following preliminary conclusions:

(1) We note that the 8498 Å line is much weaker than the other two lines of the triplet. Assuming equilibrium population of the 3^2D substates and an Einstein A value of 8.1×10^5 (Linsky, 1968), the 8498 Å line has 0.111 the opacity of the 8542 Å line and is thus formed much lower in the atmosphere.

(2) In our data the general asymmetry of the line profiles is that the red wings of the lines are higher than the blue wings. This asymmetry persists even if we allow for

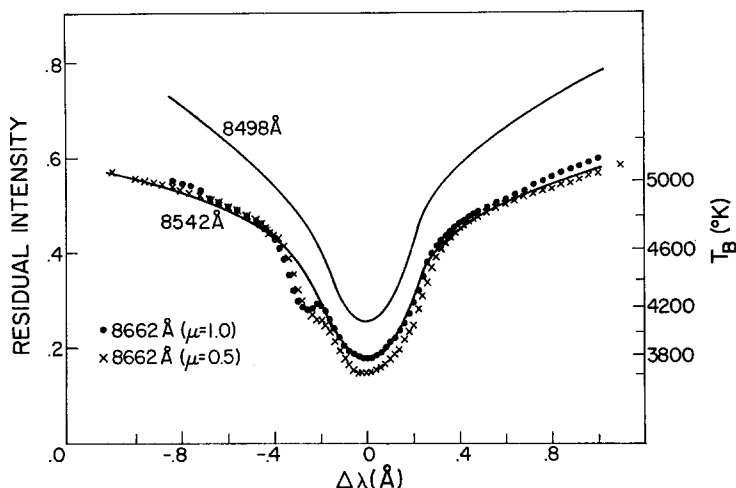


Fig. 1. Residual intensities for the Ca II lines at 8498 Å, 8542 Å, and 8662 Å at the center of the solar disk and at $\mu = 0.5$ for the 8662 Å line. Also shown are the equivalent brightness temperatures.

a 1 km/sec blue shift in the line cores when we define the line centers. This asymmetry is the opposite of that seen in the cores of the H and K lines but in the same sense as that seen in the wings of the H and K lines (White and Suemoto, 1968).

(3) Even at the high spectral resolution used in these observations the line profiles exhibit no hint of the central emission or double reversal features seen in the H and K lines in quiet regions of the chromosphere. This implies that the line source functions decrease monotonically with height at least to the point at which the lines become optically thin. Such behavior is not true of plage regions where the line profiles have central emission and absorption features or in sunspots where they have just central emission (Mustel and Tsap, 1956, 1958). In active regions the infrared line profiles and source functions thus are qualitatively similar to those of the H and K lines.

(4) Each line limb darkens at all wavelengths as do the H and K lines. This limb darkening also suggests that the line source functions decrease monotonically with height although there are alternative explanations.

(5) From Figure 1 we conclude that the emergent specific intensities of the 8542 Å and 8662 Å lines, apart from a small difference due to the different wavelengths of the lines, obey the relations

$$I(8542, \mu, \Delta\lambda) = I(8662, \mu, \Delta\lambda) \quad \text{for } |\Delta\lambda| < 0.4 \text{ \AA}, \quad (1)$$

and

$$I(8542, \mu, \Delta\lambda) = I(8662, \sim \mu/2, \Delta\lambda) \quad \text{for } |\Delta\lambda| > 0.4 \text{ \AA} \\ < 1.0 \text{ \AA}. \quad (2)$$

The 8662 Å line is 0.56 times as opaque as the 8542 Å line if the $3^2D_{3/2}$ and $3^2D_{5/2}$ states are populated in equilibrium and the spontaneous de-excitation rates are

7.2×10^6 and 7.8×10^6 , respectively, as compiled by Linsky (1968). We therefore suspect that the correct relationship for the line wings is

$$I(8542, \mu, \Delta\lambda) = I(8662, 0.56\mu, \Delta\lambda) \quad \text{for } |\Delta\lambda| > 0.4 \text{ \AA} \\ < 1.0 \text{ \AA}, \quad (3)$$

since the continuous opacity $< 5\%$ of the wing opacity at $|\Delta\lambda| = 1.0 \text{ \AA}$.

Equation (3) implies that at the large line center optical depths at which the wings are formed there is source function equality at common heights, whereas Equation (1) implies inequality at the smaller optical depths in which the line cores are formed. Jefferies and White (1967) have shown that in principle there is insufficient information in limb darkening observations of a multiplet to infer the variation of line source functions and broadening parameters with continuum optical depth. Such analyses as the previously cited work on the *D* and *b* lines are possible only in the special case of source function equality. There is thus no apparent theoretical procedure for analyzing the calcium infrared triplet.

It is interesting to consider whether the data are consistent with a plane-parallel homogeneous atmosphere and theoretical interpretations of the H and K lines. For a plane-parallel homogeneous atmosphere the line source functions depend only on height and are related to the frequency, electron temperature, and departure coefficients, b_L and b_U , for the lower and upper levels by the expression

$$S = \frac{2h\nu^3}{c^2} \left(\frac{b_L}{b_U} e^{h\nu/kT_e} - 1 \right)^{-1}. \quad (4)$$

Linsky (1968) finds the cores ($|\Delta\lambda| < 0.4 \text{ \AA}$) of the two strongest infrared lines are formed in a region where $4200 \text{ K} < T_e < 5700 \text{ K}$ and $b_L/b_U \geq 1$. Since for these temperatures $e^{h\nu/kT_e} \gg 1$, the last term may be dropped relative to the $(b_L/b_U) e^{h\nu/kT_e}$ term in Equation (4).

We wish to infer from the data the extent to which the ratio of departure coefficients for the 4^2P sublevels and the 3^2D sublevels apparently depart from unity and then consider whether these departures are physically plausible. The ratio of line source functions at a common height is approximately given by

$$\frac{S(8542)}{S(8662)} \approx \frac{I(8542, \mu, \Delta\lambda)}{I(8662, 0.56\mu, \Delta\lambda)}. \quad (5)$$

This equation will be very accurate because errors associated with the Eddington-Barbier relation should cancel out if we take a ratio and do not require that the intensity equal the source function at monochromatic optical depth of unity. Also the Eddington-Barbier relation is a good approximation when source functions vary slowly with optical depth as is true for the infrared lines. If we insert Equation (4) into Equation (5) and replace the emergent specific intensity by the product of the

residual intensity $r(\lambda, \mu, \Delta\lambda)$ and the line center continuum intensity, we obtain

$$\begin{aligned} & \frac{b(4^2P_{3/2})/b(3^2D_{5/2})}{b(4^2P_{1/2})/b(3^2D_{3/2})} \\ &= \frac{r(8542, \mu, \Delta\lambda)}{r(8662, 0.56\mu, \Delta\lambda)} \exp\left[-\frac{h}{k}(v_{8542} - v_{8662}) \times \left(\frac{1}{T_c} - \frac{1}{T_e}\right)\right] \\ &= \frac{r(8542, \mu, \Delta\lambda)}{r(8662, 0.56\mu, \Delta\lambda)} \exp\left[-234\left(\frac{1}{6055} - \frac{1}{T_e}\right)\right], \end{aligned} \quad (6)$$

where T_c is the continuum brightness temperature ($=6055$ K). The exponential term in this equation, which results from the slight difference in wavelengths of the two lines, will always be within 0.2% of unity and can be ignored. At $\mu=0.56$ we estimate the central intensity of the 8662 Å line to be 0.152, while at $\mu=1.00$ that of the 8542 Å line is 0.179. At line center the residual intensity ratio in Equation (6) is 1.18, but as shown in Figure 2 the ratio obtained using the red wing of the 8662 Å line decreases to unity at $\Delta\lambda > 0.4$ Å.

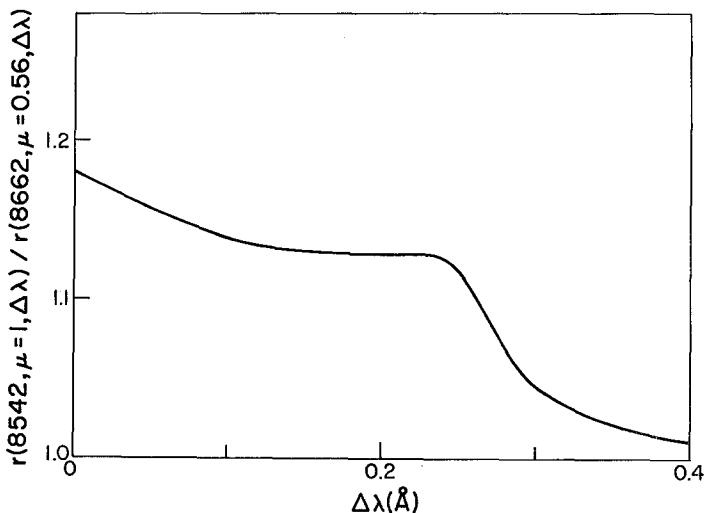


Fig. 2. The ratio of residual intensities of the 8542 Å line at the center of the disk and the red wing of the 8662 Å line at $\mu=0.56$ are given as a function of $\Delta\lambda$, the change in wavelength from the line center.

Under the assumption of a plane-parallel homogeneous atmosphere, a consistent interpretation of the data thus requires that the ratio $[b(4^2P_{3/2})/b(4^2P_{1/2})]/[b(3^2D_{5/2})/b(3^2D_{3/2})]$ be significantly larger than unity at those heights at which the line cores between -0.4 Å and $+0.4$ Å are formed. We question now whether this is physically plausible. In the previous paper Linsky (1970, Figure 6) showed that direct collisional coupling between the 4^2P substates and indirect coupling via the 3^2D states produce very nearly source function equality of the H and K lines

at common heights corresponding to K line center optical depths τ_K greater than 1. Thus the ratio $b(4^2P_{3/2})/b(4^2P_{1/2})$ is unity for $\tau_K > 1$. The chromospheric model assumed in those calculations has electron and proton densities of 3.8×10^{10} and 3.6×10^{10} , respectively, at $\tau_K = 1$. Since the fine structure collisional rate between the 4^2P sublevels is proportional to the electron and proton densities (Dumont, 1967) and since these densities are significantly lower than those suggested by the eclipse continuum and line data (Thomas and Athay, 1961; Henze, 1969), it is very unlikely that the ratio $b(4^2P_{3/2})/b(4^2P_{1/2})$ departs from unity at $\tau_K > 1$.

According to Linsky (1968) monochromatic optical depth unity in the 8542 Å line at line center and at $\Delta\lambda = \pm 0.4$ Å occurs at τ_{8542} equal to 1 and 4200, respectively, corresponding to τ_K equal to 50 and 4×10^5 . Thus we conclude that $b(4^2P_{3/2})/b(4^2P_{1/2})$ must be unity and $b(3^2D_{5/2})/b(3^2D_{3/2})$ varies between 0.85 at τ_{8542} equal to 1 and 0.99 at τ_{8542} equal to 4200.

We consider now whether these ratios are plausible. In the absence of published data on the fine structure collisional rate $C(3^2D_{5/2} \rightarrow 3^2D_{3/2})$, we estimate the coupling scale or 'conversion length' for these two levels by a heuristic argument. Following Jefferies (1968) we expect source function equality of the 8542 Å and 8662 Å lines or $b(3^2D_{5/2})/b(3^2D_{3/2})$ equal to unity at those depths at which a photon of one line is likely to escape from the atmosphere in the other line of the multiplet. Consider an 8542 Å line photon. In about one line center optical depth it excites a Ca II ion to the $4^2P_{3/2}$ level. Since the ratio of spontaneous de-excitation rates in the K and 8542 Å lines $A_K/A_{8542} \approx 20$ and $C(4^2P_{3/2} \rightarrow 4^2P_{1/2})/A_K \approx 0.02$ (cf. Linsky, 1970), the most likely transition is the emission of a K line photon. Typically 20 scatterings in the K line occur before the emission of an 8542 Å photon and 50 before a transition to the $4^2P_{1/2}$ level. From this level the creation of an 8662 Å line photon is considerably more likely than a collisional transition back to the $4^2P_{3/2}$ level. Thus, on the average, an 8542 Å photon is $2\frac{1}{2}$ times more likely to result from an interaction of our 8542 Å photon with a Ca II ion than is conversion to an 8662 Å photon. The conversion length for 8542 Å photons is thus $2\frac{1}{2}$ in τ_{8542} units. We therefore expect source function equality in the infrared lines very close to line center rather than at $\Delta\lambda = \pm 0.4$ Å as is deduced from the data. We would like to see detailed calculations based upon good values of the $C(3^2D_{5/2} \rightarrow 3^2D_{1/2})$ rate to confirm our heuristic argument.

We see two possible ways out of this apparent contradiction between theory and observation. One is to say that the data are in error. This we consider unlikely because the recent observations of De Jager and Neven (1967) are in qualitative agreement with our own and also lead to the same discrepancy. Alternatively we can ascribe the apparent source function inequality to inhomogeneities in the solar chromosphere. The profiles of the infrared lines as well as the H and K lines broaden to the limb suggesting that the Doppler half-width may be larger in the horizontal direction than in the vertical. This particular type of inhomogeneity produces limb brightening rather than darkening. Avrett and Linsky (1968) and Beebe and Johnson (1968) suggest that the intensity differences seen in spectroheliograms taken in the core of the K line

may provide a clue to limb darkening in the H and K lines. Beebe and Johnson have constructed a two-component model of the chromosphere in which the H and K line source functions decrease monotonically with height in the cooler and/or less dense component, but increase with height in the hotter and/or more dense component. These two components correspond to the dark supergranule cells and bright but narrow network between the cells. They find that as a result of the narrowness of the network optical paths through it become shorter at the limb and the composite H and K line profiles limb darken. This same chromospheric structure is seen in the cores of the infrared lines so that this mechanism should enhance the limb darkening of these lines and possibly resolve the contradiction.

Acknowledgements

The authors wish to thank Miss Sylvia Larsen for assistance in reducing some of the data and Drs. R. N. Thomas, R. C. Altrock, and O. R. White for helpful suggestions. We also acknowledge the support of the National Aeronautics and Space Administration through a grant to the University of Colorado.

References

- Athay, R. G. and Zirker, J. B.: 1962, *Astrophys. J.* **136**, 242.
 Avrett, E. H. and Linsky, J. L.: 1968, *Astron. J.* **73**, S54.
 Beebe, H. A. and Johnson, H. R.: 1968, in *Resonance Lines in Astrophysics*, National Center for Atmospheric Research, Boulder, Colo., p. 225.
 Curtis, G. W. and Jefferies, J. T.: 1967, *Astrophys. J.* **150**, 1061.
 David, K. H. and Elste, G.: 1962, *Z. Astrophys.* **54**, 12.
 Delbouille, L. and Roland, G.: 1963, *Photometric Atlas of the Solar Spectrum from $\lambda 7498$ to $\lambda 12016$* , Mem. Société Roy. de Sciences de Liège, Special Vol. No. 4.
 De Jager, C. and Neven, L.: 1967, *Bull. Astron. Inst. Neth. Supp. Series 1*, 325.
 Dumont, S.: 1967, *Ann. Astrophys.* **30**, 421.
 Henze, W., Jr.: 1969, *Solar Phys.* **9**, 65.
 Jefferies, J. T.: 1960, *Astrophys. J.*, **132**, 775.
 Jefferies, J. T.: 1968, *Spectral Line Formation*, Blaisdell, Watham, Mass., Ch. 8.
 Jefferies, J. T. and White, O. R.: 1967, *Astrophys. J.* **150**, 1051.
 Linsky, J. L.: 1968, *Smithsonian Special Report*, No. 274.
 Linsky, J. L.: 1970, *Solar Phys.* **11**, 355.
 Minnaert, M., Mulders, G. F. W., and Houtgast, J.: 1940, *A Photometric Atlas of the Solar Spectrum*, D. Schnabel, Amsterdam.
 Mohler, O. C., Pierce, A. K., McMath, R. R., and Goldberg, L.: 1962, *Photometric Atlas of the Near Infrared Solar Spectrum, $\lambda 8465$ to $\lambda 25242$* , Univ. of Mich. Press, Ann Arbor.
 Mustel, E. R. and Tsap, T. T.: 1956, *Izv. Krymsk. Astrofiz. Observ.* **16**, 67.
 Mustel, E. R. and Tsap, T. T.: 1958, *Izv. Krymsk. Astrofiz. Observ.* **20**, 74.
 Pierce, A. K.: 1964, *Appl. Optics* **3**, 1337.
 Skumanich, A.: 1969, private communication.
 Thomas, R. N. and Athay, R. G.: 1961, *Physics of the Solar Chromosphere*, Interscience Publishers, New York, Ch. 6.
 Waddell, J. H.: 1962, *Astrophys. J.* **136**, 231.
 Waddell, J. H.: 1963, *Astrophys. J.* **137**, 1210.
 White, O. R. and Suemoto, Z.: 1968, *Solar Phys.* **3**, 523.